

Mechanism of confinement in low-dimensional organic conductors

Y. Suzumura^{a,b}, M. Tsuchiizu^a

^aDepartment of Physics, Nagoya University, Nagoya 464-8602, Japan

^bCREST, Japan Science and Technology Corporation (JST)

(Received)

Confinement-deconfinement transition in quarter-filled two-coupled chains comprising dimerization, repulsive interactions and interchain hopping has been demonstrated by applying the renormalization group method to the bosonized Hamiltonian. The confinement given by the irrelevant interchain hopping occurs with increasing umklapp scattering which is induced by the dimerization leading to effectively half-filling. It is shown that the transition originates in a competition between a charge gap and the renormalized interchain hopping.

KEYWORDS: A. Organic compounds, D. Electronic structure, D. Electrical Properties

§1. Introduction

In low-dimensional organic conductors, repulsive interactions play an important role for electronic states with a gap or a pseudo gap. The anisotropy in electric conductivity is enhanced by interactions since the induced pseudo gap around the Fermi surface of a single chain precludes electrons from hopping between chains [1]. There are several arguments as to whether or not the electrons are confined to a chain by the repulsive interaction. Away from half-filling, the confinement needs a large magnitude of the interaction even for the small limit of the interchain hopping [2] since the effect of the interchain hopping is much larger than that of the intra-chain interaction. However, in the case of half-filling, the electrons can be confined by the interaction with a moderate strength due to umklapp scattering which induces the charge gap [3, 4, 5].

Bechgaard salts of organic conductors, TMTSF and TMTTF, can be regarded as effectively half-filling due to dimerization [6, 7]. The optical experiments have shown the finite Drude weight for the TMTSF salts but not for the TMTTF salts although the correlation gap exists in both salts [8]. This indicates the transition from an insulating state with the electrons confined to chains to a metallic state with deconfined electrons when the correlation gap becomes larger than the interchain hopping [9, 10]. In the present study, such a transition is elucidated by applying the renormalization group (RG) method to a model of quarter-filled two-coupled chains with dimerization.

§2. Formulation

We consider quarter-filled two-coupled chains given by

$$\mathcal{H} = - \sum_{j,\sigma,l} [t + (-1)^j t_d] (c_{j\sigma l}^\dagger c_{j+1\sigma l} + \text{h.c.})$$

$$- 2t_\perp \sum_{j,\sigma} (c_{j\sigma 1}^\dagger c_{j\sigma 2} + \text{h.c.}) + U \sum_{j,l} n_{j\uparrow l} n_{j\downarrow l}, \quad (1)$$

where t , t_\perp , t_d and U denote energies for the intrachain hopping, the interchain hopping, dimerization and on-site repulsion, respectively. $n_{j\sigma l} = c_{j\sigma l}^\dagger c_{j\sigma l}$. The quantity $c_{j\sigma l}$ denotes the annihilation operator of the electron at the j -th site of the l -th chain ($l = 1, 2$) with spin σ ($= \uparrow, \downarrow$). We use the Fourier transform, $c_{j\sigma l} = N^{-1/2} \sum_k c_{k\sigma l} \exp[ikja]$ with the total number of sites N and the lattice constant a . First, the t_d -term is diagonalized to obtain two bands in the reduced zone, $-\pi/2a < k < \pi/2a$, and the lower band becomes effectively half-filled, which band is described with fermion operators, $d_{k\sigma l}$, and is examined in the present study. Next, diagonalizing the t_\perp -term by $a_{k\sigma \pm} = (\mp d_{k\sigma 1} + d_{k\sigma 2})/\sqrt{2}$, the kinetic term is written as $\mathcal{H}_K^d = \sum_{k,\sigma,\zeta} \varepsilon(k, \zeta) a_{k\sigma\zeta}^\dagger a_{k\sigma\zeta}$ ($\zeta = \pm$) with $\varepsilon(k, \pm) = -2[t^2 \cos^2 ka + t_d^2 \sin^2 ka]^{1/2} \pm 2t_\perp$. Thus we have the following effective Hamiltonian [11]. The kinetic energy with the linearized dispersion around the Fermi surfaces, $k_{F\pm} = k_F \mp t_\perp/v_F$, is expressed as $\mathcal{H}_K^d = \sum_{k,p,\sigma,\zeta} v_F(pk - k_{F\zeta}) a_{kp\sigma\zeta}^\dagger a_{kp\sigma\zeta}$ with $p (= +, -)$ denoting right moving (left moving) electrons and $v_F = \sqrt{2}ta [1 - (t_d/t)^2] / [1 + (t_d/t)^2]^{1/2}$, in which the t_\perp -dependence of the velocity is discarded. Coupling constants of interactions corresponding to forward scattering with the same and opposite directions (g_4 and g_2), backward scattering (g_1) and Umklapp scattering (g_3) are given by $g_{1\perp} = g_{2\perp} = g_{4\perp} = Ua$, $g_3 \propto Ua(t_d/t)$ and $g_{1\parallel} = g_{2\parallel} = g_{4\parallel} = 0$ where \parallel and \perp denote interactions for the same spin and opposite spin.

Applying the bosonization method to electrons around the new Fermi points, we introduce Bose fields of phase variables, $\theta_{\rho+}$ and $\theta_{\sigma+}$ (θ_{C+} and θ_{S+}) [4, 5], which express fluctuations for the total (transverse) charge density and spin density, respectively [12]. The commutation relation with conjugate phase variables is given by $[\theta_{\nu+}(x), \theta_{\nu'-}(x')] = i\pi\delta_{\nu,\nu'} \text{sgn}(x - x')$. In terms of these

phase variables, our Hamiltonian is given by

$$\begin{aligned}
\mathcal{H} = & \sum_{\nu=\rho,\sigma,C,S} \frac{v_\nu}{4\pi} \int dx \left[\frac{1}{K_\nu} (\partial\theta_{\nu+})^2 + K_\nu (\partial\theta_{\nu-})^2 \right] \\
& + \frac{g_\rho}{4\pi^2\alpha^2} \int dx \left[\cos(\sqrt{2}\theta_{C+} - 8t_\perp x/v_F) \right. \\
& \quad \left. + \cos\sqrt{2}\theta_{C-} \right] \left[\cos\sqrt{2}\theta_S - \cos\sqrt{2}\theta_{S-} \right] \\
& + \frac{g_\sigma}{4\pi^2\alpha^2} \int dx \left[\cos(\sqrt{2}\theta_{C+} - 8t_\perp x/v_F) \right. \\
& \quad \left. - \cos\sqrt{2}\theta_{C-} \right] \left[\cos\sqrt{2}\theta_{S+} + \cos\sqrt{2}\theta_{S-} \right] \\
& + \frac{g_{1\perp}}{2\pi^2\alpha^2} \int dx \cos\sqrt{2}\theta_{\sigma+} \left[\cos(\sqrt{2}\theta_{C+} - 8t_\perp x/v_F) \right. \\
& \quad \left. - \cos\sqrt{2}\theta_{C-} - \cos\sqrt{2}\theta_{S+} - \cos\sqrt{2}\theta_{S-} \right] \\
& - \frac{g_3}{2\pi^2\alpha^2} \int dx \sin\sqrt{2}\theta_{\rho+} \left[\cos(\sqrt{2}\theta_{C+} - 8t_\perp x/v_F) \right. \\
& \quad \left. + \cos\sqrt{2}\theta_{C-} - \cos\sqrt{2}\theta_{S+} + \cos\sqrt{2}\theta_{S-} \right], \quad (2)
\end{aligned}$$

where $v_{\rho(\sigma)} = v_F[1+(-)U/\pi v_F]^{1/2}$, $K_{\rho(\sigma)} = [1+(-)Ua/\pi v_F]^{1/2}$, $v_C = v_S = v_F$, $K_C = K_S = 1$, $g_{\rho(\sigma)} = +(-)Ua$ and $g_3 = Ua(2t_d/t)/[1+(t_d/t)^2]$. The quantity α is a cut-off of the order of lattice constant. In eq. (2), there are twelve nonlinear terms rewritten as

$$\frac{g_{\nu p, \nu' p'}}{2\pi^2\alpha^2} \int dx \cos\sqrt{2}\psi_{\nu p} \cos\sqrt{2}\psi_{\nu' p'}, \quad (3)$$

where $\psi_{\nu\pm} = \theta_{\nu\pm}$ except for $\psi_{C+} = \theta_{C+} - (8t_\perp x/v_F)/\sqrt{2}$ and $\psi_{\rho+} = \theta_{\rho+} - \pi/(2\sqrt{2})$. The RG equations for $K_\nu = K_\nu(l)$, $t_\perp = t_\perp(l)$ and $G_{\nu p, \nu' p'} = G_{\nu p, \nu' p'}(l)$ are given, up to the second order, as [4, 5]

$$\begin{aligned}
\frac{d}{dl} \tilde{t}_\perp &= \tilde{t}_\perp - \frac{1}{8} K_C (G_{\rho+, C+}^2 \\
&+ G_{\sigma+, C+}^2 + G_{C+, S+}^2 + G_{C+, S-}^2) J_1(8\tilde{t}_\perp), \quad (4)
\end{aligned}$$

$$\begin{aligned}
\frac{d}{dl} K_\nu &= -\frac{1}{2\tilde{v}_\nu^2} K_\nu^2 [G_{\nu+, C+}^2 J_0(8\tilde{t}_\perp) \\
&+ G_{\nu+, C-}^2 + G_{\nu+, S+}^2 + G_{\nu+, S-}^2], \quad (5)
\end{aligned}$$

$$\begin{aligned}
\frac{d}{dl} K_C &= -\frac{1}{2} \sum_{p=\pm} [(K_C^2 J_0(8\tilde{t}_\perp) \delta_{p,+} - \delta_{p,-}) (G_{\rho+, Cp}^2 \\
&+ G_{\sigma+, Cp}^2 + G_{Cp, S+}^2 + G_{Cp, S-}^2)], \quad (6)
\end{aligned}$$

$$\begin{aligned}
\frac{d}{dl} K_S &= -\frac{1}{2} \sum_{p=\pm} [(K_S^2 \delta_{p,+} - \delta_{p,-}) (G_{\rho+, Sp}^2 \\
&+ G_{\sigma+, Sp}^2 + G_{C+, Sp}^2 J_0(8\tilde{t}_\perp) + G_{C-, Sp}^2)], \quad (7)
\end{aligned}$$

$$\begin{aligned}
\frac{d}{dl} G_{\nu+, Cp} &= [2 - K_\nu - K_C^p] G_{\nu+, Cp} \\
&- G_{\nu+, S+} G_{Cp, S+} - G_{\nu+, S-} G_{Cp, S-}, \quad (8)
\end{aligned}$$

$$\begin{aligned}
\frac{d}{dl} G_{\nu+, Sp} &= [2 - K_\nu - K_S^p] G_{\nu+, Sp} \\
&- G_{\nu+, C+} G_{C+, Sp} J_0(8\tilde{t}_\perp) \\
&- G_{\nu+, C-} G_{C-, Sp}, \quad (9)
\end{aligned}$$

$$\begin{aligned}
\frac{d}{dl} G_{Cp, Sp} &= [2 - K_C^p - K_S^{p'}] G_{Cp, Sp} \\
&- \frac{1}{\tilde{v}_\rho} G_{\rho+, Cp} G_{\rho+, Sp} - \frac{1}{\tilde{v}_\sigma} G_{\sigma+, Cp} G_{\sigma+, Sp} \quad (10)
\end{aligned}$$

where $\tilde{v}_\nu = v_\nu/v_F$ and $\tilde{t}_\perp = t_\perp(l)/v_F \alpha^{-1}$. J_n is the n -th Bessel function. The quantity l is related to energy scale ω or temperature T by $l = \ln(W/\omega)$ or $\ln(W/T)$ with $W(\equiv v_F \alpha^{-1})$ being of the order of band width. The initial condition for the RG equations are given by $K_\nu(0) = K_\nu$, $G_{\nu p, \nu' p'}(0) = g_{\nu p, \nu' p'}/2\pi v_F$ and $\tilde{t}_\perp(0) = t_\perp/(v_F \alpha^{-1})$ where $g_{C+, S+} = -g_{C-, S-} = 0$, $g_{C+, S-} = -g_{C-, S+} = -Ua$, $g_{\sigma+, C+} = -g_{\sigma+, C-} = -g_{\sigma+, S+} = -g_{\sigma+, S-} = Ua$, and $g_{\rho+, C+} = g_{\rho+, C-} = -g_{\rho+, S+} = g_{\rho+, S-} = g_3$. We take $\alpha = 2a/\pi$ [11] and discard the RG equations for the velocity v_ν .

§3. Confinement-deconfinement transition

We calculate eqs. (4)-(10) numerically by choosing U , t_d , and t_\perp as parameters.

Figure 1 shows the l -dependence of $K_\rho(l)$, $K_\sigma(l)$, $K_C(l)$, $K_S(l)$ and $t_\perp(l)$ which exhibit four gaps. With increasing l , $K_\rho(l)$ decreases to zero forming a gap in the total charge fluctuation while $K_C(l)$ increases infinity to induce a gap in the transverse charge fluctuation. Quantities $K_\sigma(l)$ and $K_S(l)$ decrease also to zero and lead to spin gaps for both the total and transverse spin fluctuations. The rapid increase of $t_\perp(l)$ comes from a fact that the term with $K_C(l)$ in the r.h.s. of eq. (4) reduces to zero due to a factor $J_1(8\tilde{t}_\perp)$. Figure 2 displays the corresponding l -dependence of coupling constants. The main figure shows coupling constants for forward and backward scatterings with $G_{C+, S+}$ (curve (1)), $-G_{C+, S-}$ (curve (2)), $G_{C-, S+}$ (curve (3)), $-G_{C-, S-}$ (curve (4)), $G_{\sigma+, C+}$ (curve (5)), $-G_{\sigma+, C-}$ (curve (6)), $G_{\sigma+, S+}$ (curve (7)) and $-G_{\sigma+, S-}$ (curve (8)) while the inset shows those for the umklapp scattering with $G_{\rho+, C+}$ (curve (9)), $G_{\rho+, C-}$

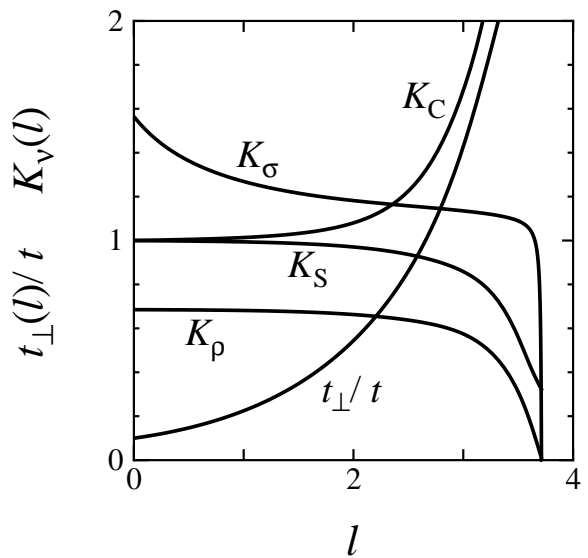


Fig. 1. The l -dependence of $K_\rho(l)$, $K_\sigma(l)$, $K_C(l)$, $K_S(l)$ and $t_\perp(l)$ for $U/t = 5$, $t_\perp/t = 0.1$ and $t_d/t = 0.05$.

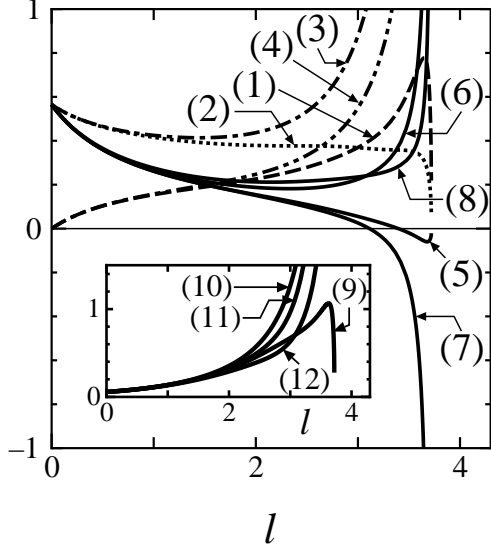


Fig. 2. The l -dependence of coupling constants $G_{\nu p, \nu' p'}(l)$ for with $U/t = 5$, $t_{\perp}/t = 0.1$ and $t_d/t = 0.05$ where curves (1)-(12) are explained in the text.

(curve (10)), $-G_{\rho+,S+}$ (curve (11)) and $G_{\rho+,S-}$ (curve (12)). Coupling constants $G_{\rho+,C-}$ and $-G_{\rho+,S+}$ increase rapidly and give rise to the trigger of relevance of the coupling constant $G_{C-,S+}$ as seen also in the one-dimensional chain. Note that the relevance of coupling constants $G_{C-,S+}$, $-G_{\sigma+,C-}$ and $-G_{\sigma+,S+}$ is also obtained in the absence of umklapp scattering [2]. The relevant behaviors found from the zero limit of K_{ρ} , K_{σ} , $1/K_C$ and K_S exhibit the phase locking of $\theta_{\rho+}$, $\theta_{\sigma+}$, θ_{C-} and θ_{S+} , which are given by $\sqrt{2}\theta_{\rho+} = \pi/2$, $\sqrt{2}\theta_{\sigma+} = 0$, $\sqrt{2}\theta_{C-} = 0$ and $\sqrt{2}\theta_{S+} = \pi$ from relevant behaviors of curves (3), (6), (7), (10) and (11). Other coupling constants, which are expected to decrease [2], are still large due to the second order perturbation. The change of the sign of $G_{\sigma+,S+}$ in the renormalization process comes from the relevance of $\theta_{\sigma+}$ and θ_{S+} . The effect of t_{\perp} on coupling constants becomes large at low energies where the splitting of magnitudes becomes noticeable for the forward scattering (between curves (1) and (4) and between curves (2) and (3)), the backward scattering (curves (5), (6), (7) and (8)), and the umklapp scattering (curves (9), (10), (11) and (12)).

In Fig. 3, the l -dependence of t_{\perp} is shown for the fixed $t_d/t = 0.05$, $t_{d,c}/t (\simeq 0.082)$ and 0.1. The increase of t_d leads to the suppression of $t_{\perp}(l)$. The case of $t_d/t = 0.05$ shows the relevant behavior, which corresponds to deconfinement. The quantity $t_{\perp}(l)$ for $t_d/t = 0.1$ does not increase monotonically but decreases to zero after taking a maximum indicating confinement. The quantity $t_{\perp}(l)$ with a critical magnitude of $t_d = t_{d,c}$ denotes the behavior between the confinement and the deconfinement. For comparison, we show the dotted curve (the dashed) curve which is calculated for $U = 0$ ($U/t = 5$, $t_d/t = 0.05$ but $g_3 = 0$ as a special choice of parameter) where the analytical expression for the dotted curve is given

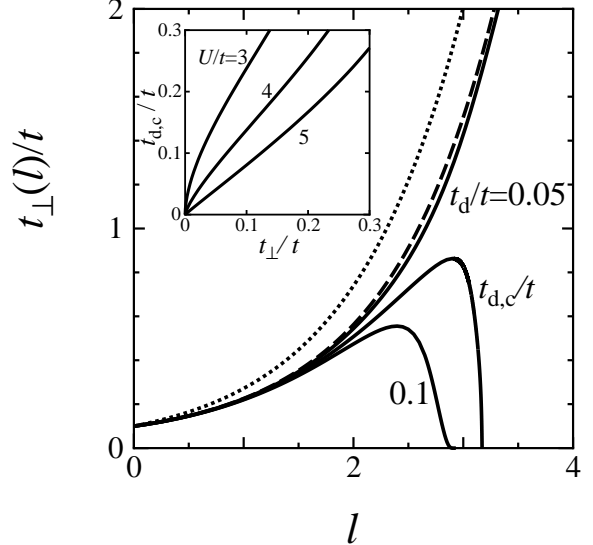


Fig. 3. The l -dependence of $t_{\perp}(l)$ for $U/t = 5$ and $t_{\perp}/t = 0.1$ with the fixed $t_d/t = 0.05$, $t_{d,c}/t (\simeq 0.082)$ and 0.1. The dotted (dashed) curve shows $t_{\perp}(l)$ for $U = 0$ ($U/t = 5$, $t_d/t = 0.05$ but $g_3 = 0$). The inset denotes $t_{d,c}$ as the function of t_{\perp} for the fixed $U/t = 3$, 4, and 5.

by $t_{\perp}(l) = t_{\perp}e^l$. Note that the dashed curve is different from the case of $U/t = 5$ and $t_d = 0$. The dashed curve is evaluated to obtain $t_{\perp}^{\text{eff},0}$, which denotes the interchain hopping renormalized only by the intrachain interaction, i.e., without the umklapp scattering. The effective interchain hopping $t_{\perp}^{\text{eff},0}$ is defined by $t_{\perp}^{\text{eff},0} = t \exp[-l_{\text{eff},0}]$ where $t_{\perp}(l_{\text{eff},0})/t = 1$ for $g_3 = 0$. The quantity $t_{\perp}^{\text{eff},0}/t$ becomes unity for $U = 0$ or $t_{\perp}/t = 1$. The inset denotes the t_{\perp} -dependence of $t_{d,c}$ for the fixed $U/t = 3$, 4, and 5.

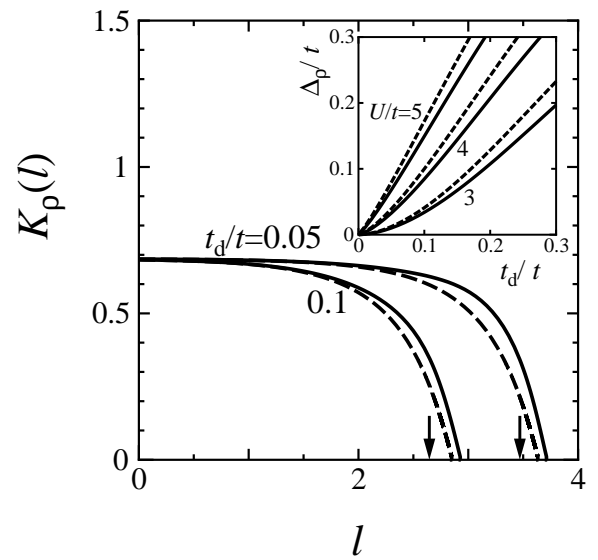


Fig. 4. The l -dependence of $K_{\rho}(l)$ for $U/t = 5$ with the fixed $t_d/t = 0.05$ and 0.1 where $t_{\perp} = 0$ for the dashed curve and $t_{\perp} = 0.1$ for the solid curve. The arrow denotes l_{Δ} defined by $K_{\rho}(l_{\Delta}) = K_{\rho}/2$. The inset exhibits the charge gap: Δ_{ρ}^{1D} for $t_{\perp}/t = 0$ (dashed curve) and Δ_{ρ} for $t_{\perp}/t = 0.1$ (solid curve).

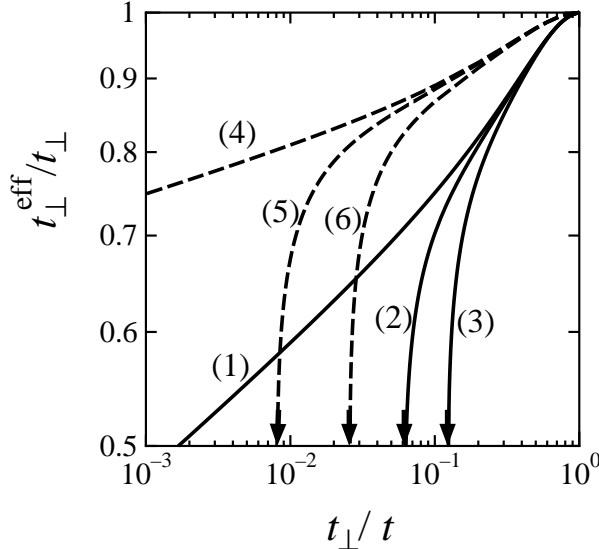


Fig. 5. The t_{\perp} -dependence of t_{\perp}^{eff} with $U/t = 3$ (dashed curve) and 5 (solid curve) where $t_d/t = 0$ (curves (1) and (4)), 0.05 (curves (2) and (5)) and 0.1 (curves (3) and (6)).

The boundary between confinement ($t_d > t_{d,c}$) and deconfinement ($t_d < t_{d,c}$) depends appreciably on U , which gives rise to the enhancement of the confined region on the plane of t_{\perp} and $t_{d,c}$. The limiting form for small t_{\perp} is given by $t_{d,c}/t \propto (t_{\perp}/t)^F$ with the U -dependent F .

The l -dependence of $K_{\rho}(l)$ is shown by solid curve for the fixed $t_d/t = 0.05$ and 0.1 in Fig. 4. The charge gap is defined by $\Delta_{\rho} = v_F \alpha^{-1} \exp[-l_{\Delta}]$ with $K_{\rho}(l_{\Delta}) = K_{\rho}/2$ and $v_F \alpha^{-1} = t(\pi/\sqrt{2})[1 - (t_d/t)^2]/[1 + (t_d/t)^2]^{1/2}$. The dashed curve, which denotes $K_{\rho}(l)$ for $t_{\perp} = 0$, leads to the charge gap, $\Delta_{\rho}^{\text{1D}}$, for one-dimensional (1D) case in the presence of dimerization, t_d . The charge gap is suppressed slightly by the interchain hopping since $K_{\rho}(l)$ for the solid curve decreases slowly compared with that for the dashed curve, i.e., l_{Δ} is increased by t_{\perp} . Such a behavior is understood from eq. (5) with $\nu = \rho$, in which the first term of the r.h.s. becomes small due to the Bessel function suppressed by the large t_{\perp} . The inset exhibits the charge gap as a function of t_d with the fixed $U/t = 3, 4$ and 5 where the solid (dashed) curve corresponds to the case of $t_{\perp}/t = 0.1$ (0). Note that the dashed curve is given by $\Delta_{\rho}^{\text{1D}} \simeq W(g_3/W)^{1/(2-2K_{\rho})}$ [10].

In Fig. 5, the t_{\perp} -dependence of t_{\perp}^{eff} with $U/t = 5$ ($U/t = 3$) is shown by the solid (dotted) curve for $t_d/t = 0$ (1), 0.05 (2) and 0.1 (3) ($t_d/t = 0$ (4), 0.05 (5) and 0.1 (6)), where the effective interchain hopping t_{\perp}^{eff} , including the effect of the dimerization, is estimated by $t_{\perp}^{\text{eff}} = t \exp[-l_{\text{eff}}]$ with $t_{\perp}(l_{\text{eff}})/t = 1$ [13]. The curves (1) and (4) for small t_{\perp}/t well reproduce the analytical result given by $t_{\perp}^{\text{eff}}/t_{\perp} \propto (t_{\perp}/t)^{\alpha_0/(1-\alpha_0)}$ with the U -dependent quantity $\alpha_0 = (K_{\rho} + K_{\rho}^{-1} + K_{\sigma} + K_{\sigma}^{-1} - 4)/4$ [1]. Comparing the slope of curve (1) with that of curve (4), one finds that the renormalization of t_{\perp} increases by the intrachain interaction U . With decreasing t_{\perp}/t , the ratio $t_{\perp}^{\text{eff}}/t_{\perp}$ decreases rapidly and becomes zero for t_{\perp}

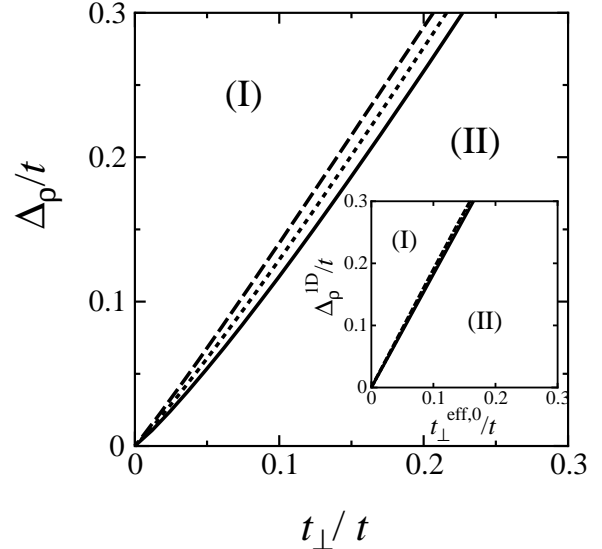


Fig. 6. The phase diagram of confinement (I) and deconfinement (II) on the plane of t_{\perp} and Δ_{ρ} for $U/t = 3$ (dashed curve), 4 (dotted curve) and 5 (solid curve). The inset denotes the corresponding phase diagram on the plane of $t_{\perp}^{\text{eff},0}/t$ and $\Delta_{\rho}^{\text{1D}}$.

less than a critical value of t_{\perp} indicated by the arrow.

From the inset of Fig. 3 and that of Fig. 4, we obtain the phase diagram of confinement (I) and deconfinement (II) on the plane of t_{\perp} and Δ_{ρ} . In Fig. 6, the boundary between these two states is shown for $U/t = 3$ (dashed curve), 4 (dotted curve) and 5 (solid curve). The boundary is rather straight and the U -dependence becomes small compared with that of the inset of Fig. 3. It has been claimed previously that such a behavior indicates the competition between the charge gap and the interchain hopping t_{\perp} [4, 5, 11]. However such a statement is not clear enough since the boundaries depend on the choice of U . This problem can be remedied by the following treatment. We take $\Delta_{\rho}^{\text{1D}}(t_{\perp}^{\text{eff},0})$ in stead of $\Delta_{\rho}(t_{\perp})$ as the vertical (horizontal) axis on the phase diagram where $\Delta_{\rho}^{\text{1D}}$ is obtained from the dashed curve of the inset of Fig. 4. The resultant boundaries are shown in the inset of Fig. 6, where the good coincidence is obtained among these three curves. Thus it is concluded that the boundary between confinement and deconfinement is determined by the competition between the one-dimensional charge gap (i.e., in the absence of the interchain hopping) and the interchain hopping renormalized only by the intrachain interaction (i.e., without the umklapp scattering).

§4. Discussion

We have examined the mechanism of confinement in terms of quarter-filled two-coupled chains with dimerization as a model of low dimensional systems. The confinement occurs when the charge gap induced by the umklapp scattering becomes larger than the interchain hopping renormalized by the intrachain hopping. It has been found that the ratio for $U/t = 5$ ($U/t = 3$) and $0.05 <$

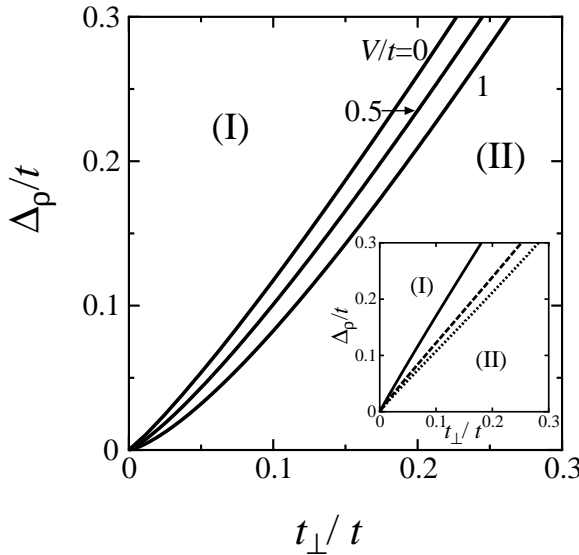


Fig. 7. The phase diagram of confinement (I) and deconfinement (II) on the plane of t_\perp and Δ_ρ . The main figure denotes the boundary for $U/t = 5$ and $t_d/t = 0.05$ with the fixed nearest-neighbor interaction: $V/t = 0, 0.5$ and 1 . In the inset, the dotted (dashed) curve denotes the boundary for the fixed $t_d/t = 0.05$ (0.1) while the solid curve denotes the boundary for the another case of the Hubbard model at half-filling with $t_d/t = 0$.

$t_\perp/t < 0.2$ is given by $\Delta_\rho^{1D}/t_\perp^{\text{eff},0} \simeq 1.8$ ($\Delta_\rho^{1D}/t_\perp^{\text{eff},0} \simeq 1.9$) and $1.1 \lesssim \Delta_\rho/t_\perp \lesssim 1.3$ ($1.3 \lesssim \Delta_\rho/t_\perp \lesssim 1.5$).

Here we discuss the effect of nearest neighbor interaction (V), for the small V , in which the commensurability energy may be negligibly small [14, 15]. In this case, V does not contribute to both the backward scattering and the umklapp scattering even in the presence of the dimerization (t_d). The effect of V appears in the forward scattering where the coupling constant is expressed as $g_{2\parallel} = g_{4\parallel} = 2Va$ and $g_{2\perp} = g_{4\perp} = (U + 2V)a$. In Fig. 7, the boundary of confinement-deconfinement transition with $U/t = 5$ is shown for $V/t = 0, 0.5$ and 1 where V enhances the confined region.

Finally we comment on the case of two-coupled chain with the conventional half-filled Hubbard model where the phase diagram is shown in the inset of Fig. 7. Compared with those of Fig. 6, the ratio Δ_ρ/t_\perp ($\simeq 1.7$ for $t_\perp/t = 0.1$) is slightly large and the boundary (solid curve) is rather straight. Such a result is compared with the boundaries for the fixed $t_d/t = 0.05$ and 0.1 , which are shown by the dotted curve and dashed curve, respectively. With increasing the dimerization, the slope of the boundary becomes steep and moves toward the solid curve since the large dimerization may lead the system to half-filling.

Acknowledgements

This work was supported by a Grant-in-Aid for Scientific Research from the Ministry of Education, Science, Sports and Culture (Grant No.09640429), Japan.

- [1] C. Bourbonnais, Mol. Cryst. Liq. Cryst. **119** (1985) 11.
- [2] M. Fabrizio, Phys. Rev. B **48** (1993) 15838.
- [3] C. Bourbonnais, in *Strongly Interacting Fermions and High T_c Superconductivity*, B. Douçot and J. Zinn-Justin, Eds. (Elsevier, Amsterdam, 1995), p. 307.
- [4] Y. Suzumura, M. Tsuchiizu, G. Grüner, Phys. Rev. B **57** (1998) R15040.
- [5] M. Tsuchiizu, Y. Suzumura, Phys. Rev. B **59** (1999) 12326.
- [6] K. Bechgaard, D. Jérôme, Physica Scripta **39** (1991), 37.
- [7] T. Ishiguro and K. Yamaji, *Organic Superconductors*, Springer Series in Solid-State Sciences (Springer-Verlag, Berlin, 1990), Vol. 88.
- [8] V. Vescoli, L. Degiorgi, W. Henderson, G. Grüner, K. P. Sarkey, L. K. Montgomery, Science **281** (1998) 1181.
- [9] J. Moser, M. Gabay, P. Auban-Senzier, D. Jérôme, K. Bechgaard, J. M. Fabre, Eur. Phys. J. B **1** (1998) 39.
- [10] A. Schwartz, M. Dressel, G. Grüner, V. Vescoli, L. Degiorgi, T. Giamarchi, Phys. Rev. B **58** (1998) 1261.
- [11] M. Tsuchiizu, Y. Suzumura, *Proc. Int. Conf. SCES '99, Nagano 1999*, to be published in Physica B,
- [12] Y. Suzumura, Prog. Theor. Phys. **61** (1979) 1.
- [13] M. Tsuchiizu, Y. Suzumura, T. Giamarchi, Prog. Theor. Phys. **101** (1999) 763.
- [14] F. Mila, X. Zotos, Europhys. Lett. **24** (1993) 133.
- [15] T. Tsuchiizu, H. Yoshioka, Y. Suzumura, *Proc. Int. Conf. 22 th Low Temp. Phys., Helsinki 1999*, to be published in Physica B